

1 **Title:** Implications of epigenetic drift in colorectal neoplasia

2 **Running title:** Implications of epigenetic drift in colorectal neoplasia

3 **Authors:** Georg E. Luebeck^{1*}, William D. Hazelton^{1*}, Kit Curtius², Sean K. Maden³, Ming Yu³,
4 Kelly T. Carter³, Wynn Burke⁴, Paul D. Lampe^{5,6}, Christopher I. Li^{7,8}, Cornelia M. Ulrich⁹, Polly A.
5 Newcomb^{8,10}, Maria Westerhoff¹¹, Andrew M. Kaz^{3,4,12}, Yanxin Luo^{13,14}, John M. Inadomi^{4,15},
6 William M. Grady^{3,4,15}

7 **Institutions:** (1) Program in Computational Biology, Fred Hutchinson Cancer Research Center,
8 Seattle, WA, 98109. (2) Centre for Tumour Biology, Barts Cancer Institute, London, UK. (3)
9 Clinical Research Division, Fred Hutchinson Cancer Research Center, Seattle, WA, 98109. (4)
10 Department of Medicine, Division of Gastroenterology, University of Washington, Seattle, WA,
11 98195. (5) Molecular Diagnostics, Public Health and Human Biology Divisions, Fred Hutchinson
12 Cancer Research Center, Seattle, WA, 98109. (6) School of Public Health and Community
13 Medicine, University of Washington, Seattle, WA, 98195. (7) Translational Research Program,
14 Public Health Sciences Division, Fred Hutchinson Cancer Research Center, Seattle, WA,
15 98109. (8) Epidemiology, School of Public Health, University of Washington, Seattle, WA,
16 98195. (9) Huntsman Cancer Institute and Department of Population Health Sciences,
17 University of Utah, Salt Lake City, UT, 84112. (10) Cancer Prevention Program, Public Health
18 Sciences Division, Fred Hutchinson Cancer Research Center, Seattle, WA 98109. (11)
19 Department of Pathology, University of Michigan, Ann Arbor, MI, 48104. (12) Gastroenterology
20 Section, VA Puget Sound Health Care System, Seattle, WA. 98108. (13) Department of
21 Colorectal Surgery, the Sixth Affiliated Hospital of Sun Yat-Sen University, Guangzhou China.
22 (14) Gastrointestinal Institute, Sun Yat-Sen University, Guangzhou China. (15) GI Cancer
23 Prevention Program, Seattle Cancer Care Alliance, Seattle, WA, 98109.

24

25 ***Corresponding authors:**

26 E. Georg Luebeck, gluebeck@fredhutch.org; William D. Hazelton, hazelton@fredhutch.org

27 Program in Computational Biology, Fred Hutchinson Cancer Research Center, Seattle,
28 Washington, 98109;

29 **Keywords:** epigenetic drift, tissue age, DNA methylation, CpG-islands (CGIs), gene
30 expression, adenoma-carcinoma sojourn time, colorectal cancer (CRC), multistage clonal
31 expansion (MSCE) model of colorectal cancer.

32 **Financial Support:** This research was supported by the following grants: NIH grants
33 U01CA182940 (G.E. Luebeck, W.D. Hazelton, W.M. Grady, S.K. Madden, K. Curtius),
34 U01CA199336 (G.E. Luebeck, W.D. Hazelton); Barts Charity grant 472-2300, London (K.
35 Curtius) and UK Medical Research Council Rutherford fellowship (K. Curtius); and NIH grants
36 (P30CA15704, U01CA152756, R01CA194663, R01CA220004, U54CA143862, P01CA077852),
37 R.A.C.E. Charities, Cottrell Family Fund, R03CA165153, Listwin Family Foundation, Seattle
38 Translational Tumor Research program, Fred Hutchinson Cancer Research Center (S.K.
39 Madden, M. Yu, K.T. Carter, and W.M. Grady), R01CA189184 (C. Lee, C.M. Ulrich, S.K.
40 Madden, M. Yu, K.T. Carter, and W.M. Grady), R01CA112516, R01CA114467, R01CA120523
41 (C.M. Ulrich, S.K. Madden, M. Yu, K.T. Carter, and W.M. Grady), Huntsman Cancer
42 Foundation, U01 CA206110, R01CA189184 R01CA 207371 and P30CACA042014 (C.M.
43 Ulrich). U24CA074794 (P.A. Newcomb, S.K. Madden, M. Yu, K.T. Carter, and W.M. Grady).

44 This material is the result of work supported in part by resources from the VA Puget Sound
45 Health Care System and the ColoCare Study. The views expressed in this article are those of
46 the authors and do not necessarily represent the views of the Department of Veterans Affairs.

47 **Conflict of interest statement.** The authors declare no potential conflicts of interest.

48

49 **Abstract**

50 Many normal tissues undergo age-related drift in DNA methylation, providing a quantitative
51 measure of tissue age. Here we identify and validate 781 CpG-islands (CGI) that undergo
52 significant methylomic drift in 232 normal colorectal tissues and show that these CGI continue to
53 drift in neoplasia while retaining significant correlations across samples. However, compared
54 with normal colon, this drift advanced (~3-4 fold) faster in neoplasia, consistent with increased
55 cell proliferation during neoplastic progression. The observed drift patterns were broadly
56 consistent with modeled adenoma-carcinoma sojourn time distributions from colorectal cancer
57 (CRC) incidence data. These results support the hypothesis that, beginning with the founder
58 premalignant cell, cancer precursors frequently sojourn for decades before turning into cancer,
59 implying that the founder cell typically arises early in life. At least 77-89% of the observed drift
60 variance in distal and rectal tumors was explained by stochastic variability associated with
61 neoplastic progression, while only 55% of the variance was explained for proximal tumors.
62 However, gene-CGI pairs in the proximal colon that underwent drift were significantly and
63 primarily negatively correlated with cancer gene expression, suggesting that methylomic drift
64 participates in the clonal evolution of CRC. Methylomic drift advanced in colorectal neoplasia
65 consistent with extended sojourn time distributions, which accounts for a significant fraction of
66 epigenetic heterogeneity in CRC. Importantly, these estimated long-duration premalignant
67 sojourn times suggest that early dietary and lifestyle interventions may be more effective than
68 later changes in reducing CRC incidence.

69

70 **Statement of Significance**

71 Findings present age-related methylomic drift in colorectal neoplasia as evidence that
72 premalignant cells can persist for decades before becoming cancerous.

73

74 **Introduction**

75 Colorectal cancers (CRC) arise along alternative pathways through an accumulation of
76 mutations and epigenetic alterations accompanied by clonal expansions, along with random and
77 selective drift (1-5). Several mutations or epigenetic changes are thought to be necessary (e.g.
78 bi-allelic inactivation of *APC*, epigenetic silencing of *MLH1*) to initiate premalignant clonal growth
79 (6). Occult premalignant clones that do not undergo extinction may grow into observable
80 adenoma while accumulating (epi)genetic alterations, with some developing genomic instability,
81 undergoing malignant transformation and invasive growth (7-9). Rates for these processes may
82 be influenced by obesity, diet, genetics, the microbiome and other factors (3, 10-12). Although
83 CRC genomes have been extensively profiled for somatic mutations, chromosomal
84 abnormalities and epigenetic alterations (3, 9), little is known about the dynamics of the
85 carcinogenic process, including the sojourn time distribution from the time when a premalignant
86 founder cell is born to when the descendent cancer becomes clinically identifiable (13). Here we
87 aim to better understand these dynamics and the role of epigenetic drift in the colon and rectum
88 as an indicator of tissue aging and its potential phenotypic effects in colorectal neoplasia (14-
89 16).

90 Recently, we established a key role of differential *methylomic drift* in the progression of
91 Barrett's esophagus (BE) to esophageal adenocarcinoma (EAC) by analyzing age-related
92 differences in DNA methylation between normal esophageal epithelium, metaplastic BE tissue
93 and EAC tissue (17, 18). Here we define methylomic, or epigenetic, drift to represent the tissue-
94 specific and age-related increases in DNA methylation at certain CpG dinucleotides. One major
95 finding of this earlier analysis was that epigenetic drift is widespread in BE genomes with the
96 magnitude of drift being highly variable between individuals, suggesting significant differences in
97 BE tissue age. We also observed a significant negative correlation of advanced methylomic drift
98 at the CpG-island (CGI) level with the expression of 200 genes, including several genes that

99 have recently been proposed as diagnostic markers for BE or have been implicated in
100 esophageal carcinogenesis (19, 20).

101 Epigenetic drift in the colon has been previously identified at a number of genes, in
102 particular at promoter-associated CpG island (CGI) (14, 21-23). However, methylomic tissue
103 aging has only recently been studied more extensively in colon, using advanced statistical
104 regression methods (24, 25) applied to data from high-throughput techniques such as reduced
105 representation bisulfite sequencing (RRBS) and high-density DNA-methylation arrays.

106

107 **Materials and methods**

108 In this study, we used a conventional regression approach geared toward a fuller assessment of
109 methylomic drift both at the single CpG and CGI level and, for the first time, provide a genome-
110 wide evaluation of methylomic drift in colon (left/right) and rectum from normal and neoplastic
111 tissue biopsies. We evaluated methylation levels at $> 450,000$ CpG probes using the Illumina
112 HM450 beadchip array (HM450) in a total of 675 colorectal tissue samples. Of particular interest
113 were site and sex differences in methylomic drift, inter-individual heterogeneity, and whether
114 drift patterns at the probe and CGI level reflect the expected variance of tissue sojourn times in
115 the adenoma-to-carcinoma sequence. Estimates of adenoma-to-carcinoma times for rectum,
116 distal, and proximal colon for the two sexes were based on mathematical models developed by
117 our group to explain age-specific incidence patterns of CRC in the US and UK (26). (See Fig. 1).
118 Here, we derive mathematical expressions for the distribution of total sojourn times from the
119 occurrence of the premalignant founder cell to the descendent carcinoma, with these sojourn
120 times properly conditioned on the time (patient age) when the descendent carcinoma is
121 diagnosed and removed for molecular analysis.

122 Of note, the premalignant sojourn times introduced here differ from clinical adenoma
123 sojourn times (with varying estimates that range up to ~ 25 years (27)) as they capture the entire

124 phase of clonal expansion including the occult phase of the adenoma, the clinical (detectable)
125 phase, and malignant phase that leads to symptomatic cancer. Hence, the difference is that the
126 sojourn times we estimate date back to the premalignant founder cell that undergoes slow
127 stochastic growth and does not become extinct.

128 Finally, comparing CGI level methylomic drift with gene expression in CRC, we
129 addressed the question whether methylomic drift may turn into a selective force impacting gene
130 expression similar to our findings for EAC.

131 **Consortia and Patient Samples**

132 This study included normal colon and rectum samples obtained from patients participating in
133 various studies in the Seattle-Puget Sound region, including the Luo Study (2), the Seattle
134 ColoCare Study (28), the Screening Marker Study (SMS) (29), and GICaRes (GICR) (30).
135 Written informed consent was obtained from all patients, the studies were conducted in
136 accordance with recognized ethical guidelines (e.g., Declaration of Helsinki, CIOMS, Belmont
137 Report, U.S. Common Rule) and the studies followed protocols approved by various Institutional
138 Review Boards. (See Table 1).

139 **Experimental Plan/Study Design**

140 For discovery, we utilized SMS tissue samples (n=150) to identify significant DNA methylation
141 drift (q-value $< 10^{-4}$) at the CpG probe level. Tissue samples (n=68, left colon; n=14, right colon)
142 from the independent GICR study were used to validate the discovered drift-CpGs, including
143 analyses of drift differentials by sex and colorectal location both at the single CpG dinucleotide
144 and CpG-island (CGI) level (with *drift-CGIs* defined as containing at least 5 drift CpGs per
145 island). Next, we obtained methylation data from endoscopic normal and cancer samples
146 published by Luo et al. (2, 31) and The Cancer Genome Atlas (TCGA) consortium Colorectal
147 Adenocarcinoma (COAD) and Rectum Adenocarcinoma (READ) projects (32, 33) to evaluate
148 drift-related methylation patterns in neoplastic tissues. The TCGA data also included information

149 on the percentage of tumor cells that we used to adjust measured drift levels in the tumors for
150 normal, stromal and necrotic cell content. For TCGA data, we accessed the data via the
151 Genomic Data Commons (level 1 HM450 methylation array idats) and for gene expression data
152 via Firehose (Level 3, v2 pipeline, RSEM-normalized Illumina HiSeq 2000 gene expression
153 counts, <http://gdac.broadinstitute.org/>, (34). All methylation array data were preprocessed as
154 described in SI.

155 **Statistical software and data metrics**

156 Data pre-processing and most analyses were performed using the R programming language
157 (v3.4.4) (35). The minfi Bioconductor package was used to analyze methylation data and
158 preprocess idats as described previously (36).

159 Levels of DNA methylation across islands and CpGs are provided as β -values ($0 < \beta < 1$),
160 which represents the percentage of methylation at a given site or island, or as M-values,
161 calculated as ($\text{logit}_2(\beta)$). In keeping with our previous studies of methylomic drift in Barrett's
162 esophagus, we preselected CpG probes that showed low levels of methylation ($\beta < 0.5$) in
163 normal tissue samples (17). See SI for further details.

164 **Data Availability**

165 Methylation data used in this study is deposited on the Gene Expression Omnibus, accession
166 GSE113904. All other data were previously published in open-access repositories.

167 **Adenoma-to-carcinoma sojourn time distributions**

168 We previously published estimates for the mean sojourn time of an adenoma (from the birth of
169 its founder cell) to cancer (13, 37). However, to correlate the methylomic drift in tumor tissue
170 samples with tissue age, it is necessary to condition the estimate on the age when the cancer
171 tissue sample was collected, while calculating the sojourn time as beginning with the initiating
172 event that leads to the first premalignant cell that generates an adenoma and eventually the

173 cancer from which the tissue sample was collected. This is typically close to the patient age at
174 the time of diagnosis. Here we provide a derivation of the sojourn time distribution conditioned
175 on the age cancer is detected. Additional mathematical details can be found in previously
176 published articles (38, 39).

177 Given the age a cancer is detected clinically, two random events are assumed to occur
178 prior to detection: (1) Initiation of a viable (pre-malignant) adenoma (referred to as a *p-clone*) that
179 does not become extinct by the time it transforms to cancer and (2), a malignant transformation
180 in the clonally expanding *p-clone*. A third event, clinical observation of the carcinoma, coincides
181 with the size-dependent detection of a malignant clone (*m-clone*) in the *p-clone* that forms the
182 cancer. Let $Y(t)$ be the (random) number of pre-malignant cells in a *p-clone* at time t and
183 $f_0(u_1 | Y(t) > 0)$ be the conditional density function for the initiation of a *p-clone* (at time u_1) that
184 is conditioned on not becoming extinct prior to malignant transformation at time t . Further, let
185 $f_{p-clone}(t - u_1)$ be the conditional density function for a *p-clone* to undergo a first malignant
186 transformation in time length $t - u_1$ that leads to a first cancer. Then, as shown in the SI, we
187 have the following expression for the conditional density function of the initiating event that
188 leads to a first malignant clone at random time $T_M = t$,

$$189 \quad f_{Ad}(u_1 | T_M = t) = \frac{f_{p-clone}(t - u_1) f_0(u_1 | Y(t) > 0)}{\int_0^t du f_{p-clone}(t - u) f_0(u | Y(t) > 0)}. \quad (1)$$

190 Here T_M represents the time when a malignant transformation occurs that will lead to a
191 viable malignant clone and a clinically detected cancer at a later (random) time $T_C = a$. To
192 account for this, we convolve the distribution in Eq. (1) over times $T_M = u_2$ for malignant
193 transformation with the probability density for clinical detection of the malignant clone (*m-clone*)
194 as a carcinoma at age $T_C = a$.

195
$$g_{Ad}(u_1 | T_C = a) = \int_{u_1}^a du_2 f_{m-clone}(a - u_2) f_{Ad}(u_1 | T_M = u_2). \quad (2)$$

196 Because multiple malignant transformations may occur during the lifetime of the
197 adenoma before it turns into cancer, this formula is an approximation. However, as was shown
198 in [13], this process can be well approximated by an effective malignant transformation in the p-
199 clone which generates a viable m-clone with transformation rate $\mu_{eff} = \mu p_\infty$, where μ is the
200 rate for malignant transformations and p_∞ is the asymptotic non-extinction probability (see SI
201 for details).

202 Explicit formulas for $f_0(u_1 | Y(t) > 0)$, $f_{p-clone}(t - u_1)$, $f_{m-clone}(t - u_2)$, are provided in
203 Supplemental Information (SI) (see Eqs S9, S11, and S13). The distribution of the adenoma
204 initiation time u_1 given in Eq. (2) can then be used to compute the expected adenoma-to-
205 carcinoma sojourn times $E(s)$ and their variance $Var(s)$, conditioned on the carcinoma being
206 detected at age $T_C = a$. Since $s = a - u_1$, we have

207
$$E(s) = \int_0^a ds s g_{Ad}(a - s | T_C = a) \quad (3)$$

208
$$Var(s) = \int_0^a ds (s - E(s))^2 g_{Ad}(a - s | T_C = a). \quad (4)$$

209 **Regression modeling of tumor methylation data**

210 We used a constrained non-linear regression model, corrected for the presence of normal and
211 stromal cell fractions in the tumor samples, to fit the drift-CGI methylation levels of both TCGA
212 and Luo tumors (excluding adenomas), separately for both sexes. The observed methylomic
213 drift in these tumors was assumed to be the sum of an unobserved (true) neoplastic drift and
214 drift associated with the non-tumor (normal/stromal) cell content in the sample. Specifically, we
215 used the following model to relate the mean methylation level D across the identified 781 drift-
216 CGI to the expected premalignant sojourn time $E(s)$, corrected for the measured fractions of

217 normal/stromal cells in the tumor samples, f_N , and with a fixed offset ε representing the mean
218 level of normal methylation at birth for all drift-CGI:

$$219 \quad D = (1 - f_N) [\varepsilon + \alpha_T E(s)] + f_N [\varepsilon + \alpha_N E(a - s)]. \quad (5)$$

220 Using this model, we estimated the CGI-level drift rate α_T for the tumors, while the
221 normal drift rate α_N across the 781 CGI was independently estimated using all normal tissue
222 samples from the SMS and GICR studies. Numerical values for the parameters in Eq. (5) and
223 estimates of the tumor drift rate α_T for males and females are provided in Table S1 in the SI.

224 **Variance of drift explained by stochastic cancer model**

225 To assess how much of the observed variance in drift in the Luo and TCGA CRC data can be
226 explained by the variance associated with the stochastic colon cancer model, we computed for
227 each sample the sum of square errors $SSE = \sum (D_{obs} - D_{exp})^2$, where D_{exp} is given by Eq (5) and
228 D_{obs} the observed (mean) methylomic drift for a given sample. Thus, SSE is the sum of the
229 square residuals of the data relative to the predicted age-dependent drift, adjusted for
230 normal/stromal cell content in the tumor samples. '*Variance explained*' by the stochastic model
231 is then computed as the ratio $R = SSP/SSE$, where SSP is the sum of square errors predicted by
232 the stochastic model, i.e., $SSP = \sum (\alpha_T)^2 Var(s)$. Thus, when $R < 1$ the model cannot fully explain
233 the observed variance while for $R > 1$ the model yields a sojourn time variability that is
234 inconsistent with drift data.

235 **Computer code**

236 R-code used to derive the following results is available on
237 <https://github.com/gluebeck/Epigenetic-Drift-in-Colon>

238 **Results**

239 In this analysis, we: 1) identified and validated CpG probes that drift significantly in normal
240 colorectal tissues; 2) examined the variability of drift in neoplastic tissues vs normal tissues (Luo

241 data); 3) determined corresponding drift rates at the CpG island (CGI) level defining *drift-CGIs*
242 as CpG islands that contain at least 5 drift-CpGs; 4) compared drift rates by sex and colorectal
243 location (proximal, distal, and rectum); 5) obtained island-level drift distributions in CRCs; and 6)
244 computed the expected variability of drift observable in CRCs associated with the modeled
245 distributions of premalignant (adenoma-to-carcinoma) sojourn times, defined by the time the
246 ancestral premalignant progenitor cell is born until cancer diagnosis.

247 **Identification of methylomic drift at the CpG probe-level in normal colorectal tissue**

248 To identify age-related methylomic drift across a population of normal tissue samples, we
249 performed probe-wise linear regressions using all 150 samples (both sexes) from the SMS
250 study. Only probes with $\beta < 0.5$ across all samples were included in the discovery to select for
251 positive drift, i.e. gradual increases of DNA methylation levels with age. This resulted in a total
252 of 182,498 CpG probes being tested by regressing age (at the time of biopsy) on the
253 methylation level (M-value) measured. Among these, we identified 13,525 probes with highly
254 significant (mostly upward) drift ($q\text{-value} < 10^{-4}$) as shown in Fig. 2.

255 Furthermore, when these drift probes were evaluated separately in 41 normal tissue samples
256 and 80 neoplastic tissue samples of the Luo study (2), we found that the methylomic drift was
257 mostly associated with an increased variance in neoplastic tissues compared with normal
258 tissues (Fig.2) suggesting a high level of tissue-age related heterogeneity in the neoplasia.

259 **Validation of methylomic drift in GICR study**

260 We used 68 additional normal (left colon) samples from the GICR study (30) to validate the set
261 of drift-CpGs we identified in the SMS study (29). Although the SMS samples were exclusively
262 collected in rectum, we found that out of the 13,525 drift-CpGs identified in SMS 12,700 could
263 be validated as positively ($drift\ rate > 0$) and significantly drifting in the GICR study ($p\text{-value}$
264 < 0.05) using Pearson's correlation.

265 **Drift at the CpG-island (CGI) level**

266 Motivated by our recent findings of widespread epigenetic drift involving > 1,000 CGI in Barrett's
267 esophagus (18), we also evaluated age-related drift at the CGI level in colon and rectum.
268 Among the 12,700 CpG probes that exhibited significant positive drift in both SMS and GICR
269 data sets, we identified 871 CGI with at least 5 drift-probes per island (we will refer to such CGI
270 as *drift-CGI*). As expected, island-level methylation was also highly correlated between the drift-
271 CGI in normal tissue (mean Pearson $r=0.68$), however it was attenuated in cancers (mean
272 Pearson $r=0.42$ for left colon and rectum; $r=0.55$ for right colon in TCGA).

273 To boost the overall correlations between drift-CGI, we selected a subset of 781 CGI
274 that were consistently and significantly correlated with one another across TCGA cancers in
275 both left and right colon. This filtering improved the mean drift-CGI correlations to 0.71 for
276 normal colon, 0.46 for left colon and rectum, and 0.6 for right colon. However, we obtained
277 similar results with the full set of 871 CGI.

278 For the subset of 781 drift-CGIs, we list the genomic location, associated genes, proximity to
279 transcription start sites (*TSS200* or *TSS1500*), the number of array probes and number of
280 identified drift probes and the island-level drift rate (regression slopes) in Table S2. For
281 comparison, we also identified > 1000 CGI that do not appear to undergo methylomic drift in
282 normal colon but that may or may not drift differentially in colorectal neoplasia. We refer to this
283 comparison group as 'static-CGI'.

284

285

286 **Drift at the CpG-probe vs CGI-level**

287 While >90% of drift-CpGs identified are located within or near CGI, only 60% of all probes were
288 associated with CGI on the array (i.e., are situated on an island, shore, or shelf), which shows
289 that methylomic drift in normal colorectum (as defined here) occurs predominantly at islands.

290 Furthermore, drift rates appear to be more uniform at the island level compared with estimated
291 drift rates at the single probe level (shown as drift-rate distributions by dashed and solid lines in
292 Fig. 3 at the probe- and island-level, respectively).

293 Next, to adjust for systemic differences in methylomic drift between the sexes, we
294 performed an analysis of covariance (ANCOVA) allowing for differences in drift rates by gender
295 (SMS and GICR left colon data, comparing 127 females and 91 males). Incremental differences
296 in drift rates between males and females were statistically significant for 759 of 781 drift islands
297 tested (q -value < 0.05) and are shown by their distinct distributions for males and females in
298 Fig. 3.

299 **Validating CGI level drift by gender and site**

300 Using ANCOVA regression with sex as a categorical variable and age as the continuous
301 independent variable, we were able to validate island-level drift first identified in the SMS study.
302 The GICR study comprised a total of 68 normal tissue samples from the left colon (31 males, 37
303 females) and 14 normal tissue samples from the right colon (11 males, 3 females).

304 All GICR samples were from cancer-free patients at the time of biopsy. Fig. 4 shows the
305 estimated drift rates for the two studies by gender. The drift rate distributions for males and
306 females in the left colon are clearly distinct for the two sexes with males showing 40% (SMS)
307 and 65% (GICR) higher mean drift rates compared with females. Due to small sample size, only
308 results for males and females combined are shown in Fig. 4 for methylomic drift in right
309 (proximal) colon (gray symbols).

310

311 **Methylomic drift in neoplastic tissues**

312 The expected sojourn times $E(s)$ of the parental adenoma that led to the clinically detected
313 cancers and measured methylation drift rates (adjusted for tissue composition) are shown for
314 males in Fig. 5A and 5B, respectively, by age and anatomical site together with their 95%

315 confidence bands. Similarly, Fig. 5C and 5D show female expected parental adenoma sojourn
316 times and adjusted methylation drift rates, respectively. The parameters used for these
317 predictions are taken from Meza *et al.* (26) who fitted 3-stage clonal expansion models to
318 colorectal incidence data in the US and the UK. Although the model parameters (adjusted for
319 secular trends) were similar for the US and UK, we chose to use the model parameters obtained
320 for the UK population, which historically had lower colorectal screening utilization than the US,
321 therefore better reflect the natural history of CRC. Note, the computed age-specific sojourn
322 times do not differ significantly between males and females for neoplasia in right (proximal)
323 colon and rectum. For neoplasia in left (distal) colon we obtained sojourn times that are between
324 those for rectal and proximal colon among males (Fig. 5A) but are more similar to the sojourn
325 times in rectal colon among females (Fig. 5C). However, for all sites and the two sexes, our
326 predictions suggest that adenoma bound for cancer started early in life, most likely before the
327 age of 20. See Fig. 5A and 5C and Fig. S1 in SI.

328 To see whether our sojourn time estimates are consistent with methylomic drift patterns
329 in neoplasia, we assumed constant drift rates and fitted them by regressing drift-related
330 methylation levels (at the island-level) on patient age using the computed age-, sex- and site-
331 specific premalignant sojourn times (see Material and Methods). The estimated neoplastic drift
332 rates (M-value/year), although similar for the 3 anatomical sites, were about 12-22% higher in
333 males than females (proximal colon – females/males: 0.056/0.065, distal colon: 0.054/0.061,
334 rectum: 0.051/0.061). This difference is not unexpected since we found much stronger drift rate
335 differences between the sexes in normal colorectum (Fig. 3). Of note, (1) although the corrected
336 drift patterns shown in panels B (males) and D (females) of Fig. 5 still exhibit a high degree of
337 variability compared with the expected variance, especially for proximal (right) colon, we
338 observe that the ordering of the drift patterns and their fits closely follow the predicted ordering
339 of premalignant sojourn times in panel Fig. 5A and 5C. (2) the estimated island-level drift rates
340 that best fit the methylomic patterns shown in panel 5B (males) and panel 5D (females) are

341 similar for the 3 sites and are approximately 3 to 4-fold higher than the corresponding drift rates
342 for normal colon. (3) our estimates of a roughly 3 to 4-fold acceleration of methylomic drift in
343 colorectal neoplasia is consistent with various cell proliferation measurements (discussed
344 below) in normal colorectal epithelium vs adenoma and carcinoma, suggesting that the
345 epigenetic drift (as defined here) is likely correlated with mitotic activity (23, 40-42).

346 **Methylomic tissue age (mAge) vs drift-based sojourn time predictions**

347 Several 'universal' methylomic clocks have been introduced recently to predict biological tissue
348 age using regularized regression methods (24, 25). In contrast to the drift-based clock used for
349 this study, which scans individual CpG probes for significant correlations with age, these multi-
350 tissue-type clocks primarily rely on elastic net regressions to predict chronological age from a
351 selection of CpG probes. To compare sojourn time estimates for the TCGA samples included in
352 this study (using Eq (5)) with estimates of mAge provided by others, we computed mAge for two
353 published clocks by Horvath (Horvath 1: 353 CpGs; Horvath 2: 110 CpGs) and a clock
354 developed by Hannum et al. (71 CpGs) (24, 25). All estimates were adjusted for normal cell
355 content assuming that the normal cell fraction in the tumors contributes a term proportional to
356 patient age. Table S3 shows the correlations between our predicted sojourn times and mAge for
357 the 3 models, as well as their means and p-values for difference in mean mAge and mean $E(s)$
358 = 61 years of the 322 TCGA colorectal samples used for this comparison. We find significant
359 correlations of mAge with our predictions ($r = 0.45$, $p\text{-value} < 2.2 \cdot 10^{-16}$ for the Hannum et al.
360 clock). Moreover, upon a simple recalibration of the unadjusted mAge estimates of normal
361 tissue to closely fit patient age, this clock also predicts excessively long sojourn times. In
362 contrast, while the Horvath 110 CpG clock still provides good correlations with our sojourn time
363 predictions ($r = 0.32$, $p\text{-value} = 6.9 \cdot 10^{-9}$), the 353 CpG clock correlates only poorly ($r=0.07$, $p\text{-}$
364 $\text{value} = 0.2$).

365 **Degree of methylomic drift in cancers shows strong correlation with methylation levels in**

366 **normal tissue** To compare drift patterns at the CGI-level between normal and cancer tissue, we

367 ordered the samples by their mean methylation levels across the drift-CGI in normal colon

368 tissue (Fig. 6). The resulting heatmaps (for left colon in Fig. 6, for right colon in Fig. S2) show

369 that the base-level of methylation in normal colon is predictive of the amount of drift occurring in

370 cancers. CGI that are static (first 300 top rows) in normal colon do not drift discernibly in

371 cancers (although they can be altered). In contrast, CGI that drift in normal colon show

372 accelerated drift in cancers with increasing levels of methylation in normal tissue (Fig. S3). The

373 correlation between mean drift in normal tissue and mean drift in the cancer tissues across the

374 781 drift-related islands is 0.81 ($p\text{-value} < 2.2 \cdot 10^{-16}$). In contrast, static CGI, defined here as

375 islands that comprise at least 5 CpG probes found not to undergo drift in normal colon (drift

376 rates $< 0.002/\text{year}$, shown as light grey data points in Fig. 2), do not drift in the cancers (Fig.

377 S4).

378 **Methylomic drift and gene expression**

379 We previously found that advanced methylomic drift on some CGI associated with actively

380 transcribed genes in EAC are significantly associated with reduced gene expression and

381 possibly gene silencing (18). Thus, here we investigated whether methylomic drift in CRC is

382 similarly associated with widespread transcriptional repression. To this end, we computed the

383 Pearson correlation between methylation and gene expression (RNA-seq) and its statistical

384 significance for all gene-CGI pairs for left colon ($n = 184$, including rectum) and right colon

385 cancers ($n = 138$) from the TCGA. Out of a total of 668 identified gene-island pairs in right colon

386 we found 373 (56%) of pairs that show a significant negative Pearson correlation, while only 34

387 (5%) of pairs show a significant positive correlation ($q\text{-value} < 0.01$). In contrast, left colon

388 cancers show fewer pairs being correlated. Out of a total of 663 identified gene-CGI pairs in left

389 colon we found only 170 (26%) pairs that show a significant negative correlation, while 46 (7%)
390 pairs show a significant positive correlation ($q\text{-value} < 0.01$, see Table S4).

391 Although the overall number of correlated gene-CGI pairs in right colon is almost twice
392 the number in left colon, 78% (169/216) of the pairs in left colon are also found to be
393 significantly correlated in right colon. Furthermore, we find no significant difference in the
394 fractions of repressed vs over-expressed genes affected by drift in the right vs left colon ($p\text{-}$
395 value = 0.24, Fisher's exact test). For comparison, we identified >1000 islands that appear
396 'static' in normal colon tissue (see Fig. 2) and do not show discernible age-related drift among
397 cancers (Fig. 6 and Figs. S2 and S3). Surprisingly, 16% (19%) of these static islands in left
398 (right) colon also show strong correlations between methylation and gene expression
399 suggesting that they, albeit under stronger epigenetic control in normal tissue, can also be
400 altered in neoplasia and may participate in the clonal evolution of a cancer (see Table S5).
401 However, compared to gene-CGI pairs that are associated with methylomic drift and exhibit
402 significant methylation-gene expression correlations in the cancers, fold-changes (> 2-fold up or
403 down) in expression are less common among static pairs (<25%) compared with drift pairs (>
404 62%) in left and right colon.

405

406 **Discussion**

407 Methylomic drift appears to be widespread in normal colon and rectum, involving at least 7% of
408 CpG probes tested ($q\text{-value} < 10^{-4}$). Over 90% of these probes are found on (or near) CGI, while
409 only 64% of HM450 probes are located on or near CGI. However, among probes with $\beta < 0.5$ in
410 normal colorectum, the fraction of HM450 probes on or near islands is about 88%, similar to the
411 fraction of drift-CpGs we identified. In contrast, a study by Irizarry et al. (43) of the human colon
412 cancer methylome showed that aberrant methylation predominantly occurred at conserved

413 tissue-specific CGI shores, with hypermethylation typically enriched closer to the associated
414 CGI and hypomethylation enriched further from the associated CGI. While this finding appears
415 in conflict with our findings of drift occurring mainly on (or near) CGI, we point out that our
416 definition of CGI includes the shore regions which extend 2kb from the island boundaries. Thus,
417 the island-level drift (including shore regions) in neoplastic tissue observed in our study, is not
418 inconsistent with the tissue-specific methylation changes in cancers observed by Irizarry et al.
419 (43) and may well play an important role in the phenotypic evolution of cancer.

420

421 Several important conclusions can be drawn from our findings:

422 **(1)** Methylomic drift in normal colon continues unabated at an increased rate in neoplastic tissue
423 (about 3-4 fold faster compared with normal colon), with drift-associated methylation in proximal
424 colon showing the highest gains across the older aged (age >60) cancer population, followed by
425 distal colon and with rectum showing the lowest gains. However, the estimated drift rates for
426 neoplasia in these sites are similar which suggests that, on average, neoplastic lesions in the
427 proximal colon sojourn longer than lesions in the distal colon and rectum. This conclusion is
428 consistent with the findings from independent mathematical modeling of age-specific incidence
429 curves of CRC in the US and UK (26) that suggested significantly slower growth rates of
430 proximal adenoma compared with distal and rectal adenoma.

431 **(2)** Several studies have carefully measured cell proliferation in both normal and neoplastic
432 (adenoma) colon mucosae. The study by Kikuchi et al. (44) evaluated the *Ki-67* (*MIB-1*) cell
433 proliferation marker in normal colon, adenoma of various histology, and carcinoma. Although *Ki-*
434 *67* labeling is strongly dependent on cell position within crypts, *Ki-67* labeling in normal colon
435 was $14\% \pm 5\%$ while in adenoma *Ki-67* was $26.5\% \pm 9\%$ for low grade adenoma and
436 $35\% \pm 6\%$ for high grade adenoma in the Kikuchi *et al.* study, suggesting a 2-3-fold increase in
437 cell proliferation between normal and neoplastic colon tissue. In carcinoma, *Ki-67* labeling is

438 about 3-fold higher than normal tissue ($53\% \pm 5\%$). Similarly, the study by Baker et al. (45)
439 found 3-fold increase in the number of *Ki-67+* cells at the crypt base in adenomatous colon
440 tissue that lost APC, compared with wild-type normal colon.

441 **(3)** The computed age-dependent sojourn time distributions for proximal colon, distal colon, and
442 rectum indicate that the first premalignant cell that generates a cancer-forming adenoma
443 typically arises early in life and may take decades before developing into cancer. This
444 conjecture is supported by our analysis of methylomic drift in colorectal neoplasia relative to
445 normal colon tissue which shows that drift rates in neoplastic colon are increased similarly to
446 independently measured rates of cell proliferation in adenoma and carcinoma compared with
447 those in normal colon (44). Furthermore, an independent application of 3 universal (multi-
448 tissue-type) clocks yields similarly long time scales (~60 years) for the TCGA samples analyzed
449 in this study (Table S3) with 2 of the 3 clocks showing significant correlations with the computed
450 drift-based sojourn times.

451 **(4)** Although methylomic drift appears highly variable in the tumors (even after correction for
452 normal/stromal cell content), 55-89% of the total (island-level) variance in DNA methylation
453 observed in the tumor samples can be attributed to the stochasticity of the tumor growth
454 process and random events that lead to a cancer and its detection. Note, this range of variability
455 explained by the model does not account for any variability present in normal tissue prior to
456 adenoma initiation. However, a variance analysis of methylation levels of static CGIs in normal
457 tissues compared with variances of drift-CGI in normal and cancer tissues indicates that the
458 normal sample population has a constant (non-drift) variance of about 0.018, which increases
459 >3-fold for drift-CGI to 0.07, while in cancers this variance increases to about 0.36. Thus,
460 assuming static methylomic variability across samples approximates the variability at adenoma
461 initiation, only ~5% (0.018/0.36) of the observed drift variance across cancers may be attributed
462 to pre-existing methylomic variability in normal tissue.

463 **(5)** Consistent with findings of a recent analysis of methylomic drift in Barrett's esophagus and in
464 esophageal adenocarcinoma (18), we found that advanced methylomic drift at the islands-level
465 is frequently (> 50% in right colon, > 25% in left colon) associated with significant reductions in
466 gene expression. We identified only a small number of drift-related CGI-gene pairs for which
467 drift correlated positively with gene expression (e.g., *SIM2*, *TBX5*, see Table S4). Although our
468 analysis does not demonstrate causality, the fact that epigenetic drift of CGI in normal colon is
469 more prominently associated with transcriptional changes in colorectal neoplasia than static CGI
470 that undergo little or no drift in normal colorectum suggests a potential role of methylomic drift in
471 the clonal evolution to cancer.

472 Our study has several limitations related to the nature of the available data, their clinical
473 annotation and the methylation array platform used. In particular, the HM450 platform only
474 covers a small fraction (~1.6%) of CpGs in the human genome and has an uneven distribution
475 of CpGs at the island level. Thus, our selection of drift-CpGs is biased toward islands with a
476 larger number of array probes likely resulting in an underestimation of genome-wide methylomic
477 drift. Furthermore, we lack gene expression data for our normal tissue samples (GICR, SMS
478 and Luo study) preventing a comparative study of drift-related phenotypic changes in normal vs
479 neoplastic tissue. Although, we are able to explain up to 77-89% of the observed methylomic
480 variance of drift-CGI in distal colon and rectum, we only explain a much smaller fraction (55%)
481 of this variance in proximal colon. It is conceivable that other unaccounted factors contribute
482 differentially to the observed variance including environmental exposures, diet, microbiome,
483 immune status, cancer (epi)genetics and measurement errors. Unfortunately, most of these
484 covariates are unavailable in our data and TCGA and have not been included in the modeling of
485 the adenoma sojourn times. In spite of the limitations of the modeling and lack of further data
486 that more fully explain the observed inter-individual heterogeneity in methylomic drift in these
487 samples, our results support the hypothesis that adenoma that lead to cancer arise early in life,
488 even for CRCs that occur at advanced ages. Thus, starting chemoprevention and lifestyle

489 interventions early in life (rather than later in life) may be more effective in reducing the cancer
490 burden given our findings that cancer precursors likely sojourn for decades before turning into
491 cancer.

492 In summary, our analysis shows that age-related methylomic drift is a genome-wide
493 phenomenon that occurs in normal colon and continues at an accelerated pace in colorectal
494 neoplasia. Furthermore, we show that differences in age-related drift between normal and
495 neoplastic tissues are broadly consistent with predicted long-duration but individually variable
496 total adenoma-carcinoma sojourn times that capture approximately 55-89% of the variance of
497 drift-CGI heterogeneity in CRCs. Other factors, including those related to genetics, obesity, diet,
498 lifestyle and environmental factors and use of chemo-preventative agents such as use of non-
499 steroidal anti-inflammatory drugs (NSAIDS) may account for much of the remaining
500 heterogeneity. Importantly, the estimated long duration of premalignant sojourn times suggests
501 that CRC incidence may be reduced through early (and ideally lifelong) dietary and lifestyle
502 interventions.

503

504 **Acknowledgements**

505 We gratefully acknowledge the Luo, Seattle ColoCare, and SMS study teams, the GICR
506 biorepository team, and the study participants.

507

508

509

510

511

512

513 **References**

- 514 1. Vogelstein B, Fearon ER, Hamilton SR, Kern SE, Preisinger AC, Leppert M, Nakamura Y, White R,
515 Smits AM, Bos JL. Genetic alterations during colorectal-tumor development. *The New England journal of*
516 *medicine*. 1988;319(9):525-32. Epub 1988/09/01. doi: 10.1056/NEJM198809013190901. PubMed PMID:
517 2841597.
- 518 2. Luo Y, Wong CJ, Kaz AM, Dzieciatkowski S, Carter KT, Morris SM, Wang J, Willis JE, Makar KW,
519 Ulrich CM, Lutterbaugh JD, Shrubsole MJ, Zheng W, Markowitz SD, Grady WM. Differences in DNA
520 methylation signatures reveal multiple pathways of progression from adenoma to colorectal cancer.
521 *Gastroenterology*. 2014;147(2):418-29 e8. Epub 2014/05/06. doi: 10.1053/j.gastro.2014.04.039.
522 PubMed PMID: 24793120; PMCID: PMC4107146.
- 523 3. Borrás E, San Lucas FA, Chang K, Zhou R, Masand G, Fowler J, Mork ME, You YN, Taggart MW,
524 McAllister F, Jones DA, Davies GE, Edelmann W, Ehli EA, Lynch PM, Hawk ET, Capella G, Scheet P, Vilar E.
525 Genomic Landscape of Colorectal Mucosa and Adenomas. *Cancer Prev Res (Phila)*. 2016;9(6):417-27.
526 doi: 10.1158/1940-6207.CAPR-16-0081. PubMed PMID: 27221540.
- 527 4. Bettington M, Walker N, Clouston A, Brown I, Leggett B, Whitehall V. The serrated pathway to
528 colorectal carcinoma: current concepts and challenges. *Histopathology*. 2013;62(3):367-86. Epub
529 2013/01/24. doi: 10.1111/his.12055. PubMed PMID: 23339363.
- 530 5. Shibata D. Inferring human stem cell behaviour from epigenetic drift. *The Journal of pathology*.
531 2009;217(2):199-205. Epub 2008/11/26. doi: 10.1002/path.2461. PubMed PMID: 19031430.
- 532 6. Yang D, Zhang M, Gold B. Origin of Somatic Mutations in beta-Catenin versus Adenomatous
533 Polyposis Coli in Colon Cancer: Random Mutagenesis in Animal Models versus Nonrandom Mutagenesis
534 in Humans. *Chem Res Toxicol*. 2017;30(7):1369-75. doi: 10.1021/acs.chemrestox.7b00092. PubMed
535 PMID: 28578586.
- 536 7. Baker AM, Cereser B, Melton S, Fletcher AG, Rodriguez-Justo M, Tadrous PJ, Humphries A, Elia
537 G, McDonald SAC, Wright NA, Simons BD, Jansen M, Graham TA. Quantification of Crypt and Stem Cell
538 Evolution in the Normal and Neoplastic Human Colon. *Cell Rep*. 2014;8(4):940-7. doi:
539 10.1016/j.celrep.2014.07.019. PubMed PMID: WOS:000341573500003.
- 540 8. Tomasetti C, Marchionni L, Nowak MA, Parmigiani G, Vogelstein B. Only three driver gene
541 mutations are required for the development of lung and colorectal cancers. *P Natl Acad Sci USA*.
542 2015;112(1):118-23. doi: 10.1073/pnas.1421839112. PubMed PMID: WOS:000347447100039.
- 543 9. Cancer Genome Atlas N. Comprehensive molecular characterization of human colon and rectal
544 cancer. *Nature*. 2012;487(7407):330-7. Epub 2012/07/20. doi: 10.1038/nature11252. PubMed PMID:
545 22810696; PMCID: 3401966.
- 546 10. Comstock SS, Hortos K, Kovan B, McCaskey S, Pathak DR, Fenton JI. Adipokines and obesity are
547 associated with colorectal polyps in adult males: a cross-sectional study. *PloS one*. 2014;9(1):e85939.
548 Epub 2014/01/28. doi: 10.1371/journal.pone.0085939. PubMed PMID: 24465801; PMCID: 3895019.
- 549 11. Bastide N, Morois S, Cadeau C, Kangas S, Serafini M, Gusto G, Dossus L, Pierre FH, Clavel-
550 Chapelon F, Boutron-Ruault MC. Heme Iron Intake, Dietary Antioxidant Capacity, and Risk of Colorectal
551 Adenomas in a Large Cohort Study of French Women. *Cancer Epidemiol Biomarkers Prev*.
552 2016;25(4):640-7. doi: 10.1158/1055-9965.EPI-15-0724. PubMed PMID: 26823477.
- 553 12. Mira-Pascual L, Cabrera-Rubio R, Ocon S, Costales P, Parra A, Suarez A, Moris F, Rodrigo L, Mira
554 A, Collado MC. Microbial mucosal colonic shifts associated with the development of colorectal cancer
555 reveal the presence of different bacterial and archaeal biomarkers. *Journal of gastroenterology*. 2014.
556 Epub 2014/05/09. doi: 10.1007/s00535-014-0963-x. PubMed PMID: 24811328.

- 557 13. Luebeck EG, Curtius K, Jeon J, Hazelton WD. Impact of tumor progression on cancer incidence
558 curves. *Cancer research*. 2013;73(3):1086-96. Epub 2012/10/12. doi: 10.1158/0008-5472.CAN-12-2198.
559 PubMed PMID: 23054397.
- 560 14. Issa JPJ, Ottaviano YL, Celano P, Hamilton SR, Davidson NE, Baylin SB. Methylation of the
561 Estrogen-Receptor CpG Island Links Aging and Neoplasia in Human Colon. *Nature Genetics*.
562 1994;7(4):536-40. doi: Doi 10.1038/Ng0894-536. PubMed PMID: WOS:A1994PA83200023.
- 563 15. Galamb O, Kalmar A, Bartak BK, Patai AV, Leiszter K, Peterfia B, Wichmann B, Valcz G, Veres G,
564 Tulassay Z, Molnar B. Aging related methylation influences the gene expression of key control genes in
565 colorectal cancer and adenoma. *World J Gastroentero*. 2016;22(47):10325-40. doi:
566 10.3748/wjg.v22.i47.10325. PubMed PMID: WOS:000390172600006.
- 567 16. Issa JP. Aging and epigenetic drift: a vicious cycle. *J Clin Invest*. 2014;124(1):24-9. doi:
568 10.1172/Jci69735. PubMed PMID: WOS:000329333500006.
- 569 17. Curtius K, Wong CJ, Hazelton WD, Kaz AM, Chak A, Willis JE, Grady WM, Luebeck EG. A
570 Molecular Clock Infers Heterogeneous Tissue Age Among Patients with Barrett's Esophagus. *PLoS*
571 *Comput Biol*. 2016;12(5):e1004919. doi: 10.1371/journal.pcbi.1004919. PubMed PMID: 27168458;
572 PMCID: PMC4864310.
- 573 18. Luebeck EG, Curtius K, Hazelton WD, Maden S, Yu M, Thota PN, Patil DT, Chak A, Willis JE, Grady
574 WM. Identification of a key role of widespread epigenetic drift in Barrett's esophagus and esophageal
575 adenocarcinoma. *Clin Epigenetics*. 2017;9:113. Epub 2017/10/20. doi: 10.1186/s13148-017-0409-4.
576 PubMed PMID: 29046735; PMCID: PMC5644061.
- 577 19. Chettouh H, Mowforth O, Galeano-Dalmau N, Bezawada N, Ross-Innes C, Ma/cRae S, Debiram-
578 Beecham I, O'Donovan M, Fitzgerald RC. Methylation panel is a diagnostic biomarker for Barrett's
579 oesophagus in endoscopic biopsies and non-endoscopic cytology specimens. *Gut*. 2017. Epub
580 2017/11/01. doi: 10.1136/gutjnl-2017-314026. PubMed PMID: 29084829.
- 581 20. Cancer Genome Atlas Research N, Analysis Working Group: Asan U, Agency BCC, Brigham,
582 Women's H, Broad I, Brown U, Case Western Reserve U, Dana-Farber Cancer I, Duke U, Greater Poland
583 Cancer C, Harvard Medical S, Institute for Systems B, Leuven KU, Mayo C, Memorial Sloan Kettering
584 Cancer C, National Cancer I, Nationwide Children's H, Stanford U, University of A, University of M,
585 University of North C, University of P, University of R, University of Southern C, University of Texas
586 MDACC, University of W, Van Andel Research I, Vanderbilt U, Washington U, Genome Sequencing
587 Center: Broad I, Washington University in St L, Genome Characterization Centers BCCA, Broad I, Harvard
588 Medical S, Sidney Kimmel Comprehensive Cancer Center at Johns Hopkins U, University of North C,
589 University of Southern California Epigenome C, University of Texas MDACC, Van Andel Research I,
590 Genome Data Analysis Centers: Broad I, Brown U, Harvard Medical S, Institute for Systems B, Memorial
591 Sloan Kettering Cancer C, University of California Santa C, University of Texas MDACC, Biospecimen Core
592 Resource: International Genomics C, Research Institute at Nationwide Children's H, Tissue Source Sites:
593 Analytic Biologic S, Asan Medical C, Asterand B, Barretos Cancer H, BioreclamationIvt, Botkin Municipal
594 C, Chonnam National University Medical S, Christiana Care Health S, Cureline, Duke U, Emory U, Erasmus
595 U, Indiana University School of M, Institute of Oncology of M, International Genomics C, Invidumed,
596 Israelitisches Krankenhaus H, Keimyung University School of M, Memorial Sloan Kettering Cancer C,
597 National Cancer Center G, Ontario Tumour B, Peter MacCallum Cancer C, Pusan National University
598 Medical S, Ribeirao Preto Medical S, St. Joseph's H, Medical C, St. Petersburg Academic U, Tayside Tissue
599 B, University of D, University of Kansas Medical C, University of M, University of North Carolina at Chapel
600 H, University of Pittsburgh School of M, University of Texas MDACC, Disease Working Group: Duke U,
601 Memorial Sloan Kettering Cancer C, National Cancer I, University of Texas MDACC, Yonsei University
602 College of M, Data Coordination Center CI, Project Team: National Institutes of H. Integrated genomic
603 characterization of oesophageal carcinoma. *Nature*. 2017;541(7636):169-75. doi: 10.1038/nature20805.
604 PubMed PMID: 28052061.

- 605 21. Toyota M, Issa JP. CpG island methylator phenotypes in aging and cancer. *Seminars in cancer*
606 *biology*. 1999;9(5):349-57. Epub 1999/11/05. doi: 10.1006/scbi.1999.0135. PubMed PMID: 10547343.
- 607 22. Issa JP, Ahuja N, Toyota M, Bronner MP, Brentnall TA. Accelerated age-related CpG island
608 methylation in ulcerative colitis. *Cancer research*. 2001;61(9):3573-7. Epub 2001/04/28. PubMed PMID:
609 11325821.
- 610 23. Issa JP. Aging and epigenetic drift: a vicious cycle. *The Journal of clinical investigation*.
611 2014;124(1):24-9. Epub 2014/01/03. doi: 10.1172/JCI69735. PubMed PMID: 24382386; PMCID:
612 3871228.
- 613 24. Hannum G, Guinney J, Zhao L, Zhang L, Hughes G, Sada S, Klotzle B, Bibikova M, Fan JB, Gao Y,
614 Deconde R, Chen M, Rajapakse I, Friend S, Ideker T, Zhang K. Genome-wide methylation profiles reveal
615 quantitative views of human aging rates. *Molecular cell*. 2013;49(2):359-67. Epub 2012/11/28. doi:
616 10.1016/j.molcel.2012.10.016. PubMed PMID: 23177740; PMCID: 3780611.
- 617 25. Horvath S. DNA methylation age of human tissues and cell types. *Genome Biol*. 2013;14(10). doi:
618 Artn R115
619 Doi 10.1186/Gb-2013-14-10-R115. PubMed PMID: ISI:000329387500008.
- 620 26. Meza R, Jeon J, Renehan AG, Luebeck EG. Colorectal cancer incidence trends in the United
621 States and United Kingdom: evidence of right- to left-sided biological gradients with implications for
622 screening. *Cancer research*. 2010;70(13):5419-29. Epub 2010/06/10. doi: 10.1158/0008-5472.CAN-09-
623 4417. PubMed PMID: 20530677; PMCID: 2914859.
- 624 27. Rutter CM, Knudsen AB, Marsh TL, Doria-Rose VP, Johnson E, Pabiniak C, Kuntz KM, van
625 Ballegooijen M, Zauber AG, Lansdorp-Vogelaar I. Validation of Models Used to Inform Colorectal Cancer
626 Screening Guidelines: Accuracy and Implications. *Med Decis Making*. 2016;36(5):604-14. doi:
627 10.1177/0272989X15622642. PubMed PMID: 26746432.
- 628 28. Liesenfeld DB, Grapov D, Fahrman JF, Salou M, Scherer D, Toth R, Habermann N, Bohm J,
629 Schrotz-King P, Gigic B, Schneider M, Ulrich A, Herpel E, Schirmacher P, Fiehn O, Lampe JW, Ulrich CM.
630 Metabolomics and transcriptomics identify pathway differences between visceral and subcutaneous
631 adipose tissue in colorectal cancer patients: the ColoCare study. *Am J Clin Nutr*. 2015;102(2):433-43.
632 Epub 2015/07/15. doi: 10.3945/ajcn.114.103804. PubMed PMID: 26156741; PMCID: PMC4515859.
- 633 29. Adams SV, Newcomb PA, Burnett-Hartman AN, Wurscher MA, Mandelson M, Upton MP, Zhu LC,
634 Potter JD, Makar KW. Rare Circulating MicroRNAs as Biomarkers of Colorectal Neoplasia. *PloS one*.
635 2014;9(10). doi: ARTN e108668
636 10.1371/journal.pone.0108668. PubMed PMID: WOS:000345743700027.
- 637 30. Barault L, Amatu A, Siravegna G, Ponzetti A, Moran S, Cassingena A, Mussolin B, Falcomata C,
638 Binder AM, Cristiano C, Oddo D, Guarrera S, Cancelliere C, Bustreo S, Bencardino K, Maden S, Vanzati A,
639 Zavattari P, Matullo G, Truini M, Grady WM, Racca P, Michels KB, Siena S, Esteller M, Bardelli A, Sartore-
640 Bianchi A, Di Nicolantonio F. Discovery of methylated circulating DNA biomarkers for comprehensive
641 non-invasive monitoring of treatment response in metastatic colorectal cancer. *Gut*. 2017. Epub
642 2017/10/07. doi: 10.1136/gutjnl-2016-313372. PubMed PMID: 28982739.
- 643 31. Gene Expression Omnibus (GEO) GSE48684.
644 <https://www.ncbi.nlm.nih.gov/geo/query/acc.cgi?acc=GSE48684> Global DNA methylation alterations
645 reveal multiple pathways in the initiation and progression of colorectal cancer [Internet]. National
646 Center for Biotechnology Information (NCBI). 2014 [cited Mar 26, 2018].
- 647 32. TCGA. TCGA Research Network. See: <http://cancergenome.nih.gov/> and
648 <https://portal.gdc.cancer.gov/projects/TCGA-COAD>. Accessed 6/16/2017.
- 649 33. Grossman RL, Heath AP, Ferretti V, Varmus HE, Lowy DR, Kibbe WA, Staudt LM. Toward a Shared
650 Vision for Cancer Genomic Data. *New Engl J Med*. 2016;375(12):1109-12. doi: 10.1056/NEJMp1607591.
651 PubMed PMID: WOS:000383537100002.

- 652 34. Li B, Dewey CN. RSEM: accurate transcript quantification from RNA-Seq data with or without a
653 reference genome. *Bmc Bioinformatics*. 2011;12. doi: Artn 323
654 10.1186/1471-2105-12-323. PubMed PMID: WOS:000294361700001.
- 655 35. R Core Team. R: A language and environment for statistical computing. R. Foundation for
656 Statistical Computing, Vienna, Austria. 2013. Available from: <http://www.R-project.org/>.
- 657 36. Aryee MJ, Jaffe AE, Corrada-Bravo H, Ladd-Acosta C, Feinberg AP, Hansen KD, Irizarry RA. Minfi:
658 a flexible and comprehensive Bioconductor package for the analysis of Infinium DNA methylation
659 microarrays. *Bioinformatics*. 2014;30(10):1363-9. doi: DOI 10.1093/bioinformatics/btu049. PubMed
660 PMID: WOS:000336530000004.
- 661 37. Meza R, Jeon J, Moolgavkar SH, Luebeck EG. Age-specific incidence of cancer: Phases,
662 transitions, and biological implications. *Proc Natl Acad Sci U S A*. 2008;105(42):16284-9. Epub
663 2008/10/22. doi: 10.1073/pnas.0801151105. PubMed PMID: 18936480; PMCID: 2570975.
- 664 38. Jeon J, Meza R, Moolgavkar SH, Luebeck EG. Evaluation of screening strategies for pre-malignant
665 lesions using a biomathematical approach. *Mathematical biosciences*. 2008;213(1):56-70. Epub
666 2008/04/01. doi: 10.1016/j.mbs.2008.02.006. PubMed PMID: 18374369; PMCID: 2442130.
- 667 39. Dewanji A, Jeon J, Meza R, Luebeck EG. Number and size distribution of colorectal adenomas
668 under the multistage clonal expansion model of cancer. *PLoS Comput Biol*. 2011;7(10):e1002213. Epub
669 2011/10/25. doi: 10.1371/journal.pcbi.1002213. PubMed PMID: 22022253; PMCID: PMC3192823.
- 670 40. Beerman I, Bock C, Garrison BS, Smith ZD, Gu HC, Meissner A, Rossi DJ. Proliferation-Dependent
671 Alterations of the DNA Methylation Landscape Underlie Hematopoietic Stem Cell Aging. *Cell Stem Cell*.
672 2013;12(4):413-25. doi: 10.1016/j.stem.2013.01.017. PubMed PMID: WOS:000329569500009.
- 673 41. Teschendorff AE, West J, Beck S. Age-associated epigenetic drift: implications, and a case of
674 epigenetic thrift? *Human molecular genetics*. 2013;22(R1):R7-R15. Epub 2013/08/07. doi:
675 10.1093/hmg/ddt375. PubMed PMID: 23918660; PMCID: PMC3782071.
- 676 42. Zheng SC, Widschwendter M, Teschendorff AE. Epigenetic drift, epigenetic clocks and cancer
677 risk. *Epigenomics*. 2016;8(5):705-19. doi: 10.2217/epi-2015-0017. PubMed PMID: 27104983.
- 678 43. Irizarry RA, Ladd-Acosta C, Wen B, Wu Z, Montano C, Onyango P, Cui H, Gabo K, Rongione M,
679 Webster M, Ji H, Potash J, Sabunciyan S, Feinberg AP. The human colon cancer methylome shows similar
680 hypo- and hypermethylation at conserved tissue-specific CpG island shores. *Nat Genet*. 2009;41(2):178-
681 86. Epub 2009/01/20. doi: 10.1038/ng.298. PubMed PMID: 19151715; PMCID: PMC2729128.
- 682 44. Kikuchi Y, Dinjens WN, Bosman FT. Proliferation and apoptosis in proliferative lesions of the
683 colon and rectum. *Virchows Archiv : an international journal of pathology*. 1997;431(2):111-7. Epub
684 1997/08/01. PubMed PMID: 9293892.
- 685 45. Baker AM, Cereser B, Melton S, Fletcher AG, Rodriguez-Justo M, Tadrus PJ, Humphries A, Elia
686 G, McDonald SA, Wright NA, Simons BD, Jansen M, Graham TA. Quantification of crypt and stem cell
687 evolution in the normal and neoplastic human colon. *Cell Rep*. 2014;8(4):940-7. doi:
688 10.1016/j.celrep.2014.07.019. PubMed PMID: 25127143.

689

690

691

692

693

694 **Tables**

Study group	Number of samples	Colorectal location			Sex F/M	Mean age at diag. (range)	Sample histology	Patient status
		Rectum	Left	Right				
SMS	150	150	0	0	90/60	58.1 (31 - 79)	normal	healthy
GIcaRes	82	0	68	14	40/42	60.9 (29 - 82)	normal	healthy
Luo (normal)	41	unknown	unknown	unknown	19/22	58.4 (43 - 78)	normal	matched (n=24)
Luo (neoplasia)	80 (18 aden.)	9	27	44	54/26	60.0 (23 - 89)	adv. aden. cancer	adv. aden. cancer
TCGA	322	43	141	138	145/177	64.9 (31 - 90)	cancer	cancer

695

696 **Table 1:** Study, number of samples, sample location and mean patient age (range) used for this
697 study. Note: we excluded EACs from The Cancer Genome Atlas (TCGA) with MSI and/or
698 mucinous histology.

699 **Figure Legends**

700 **Fig. 1:** DNA methylation drift measured in a cancer tissue sample provides a measure of the
701 sojourn time between initiation of the founder premalignant cell and the cancer that arises along
702 this lineage. Premalignant clones may grow gradually for decades prior to generating an
703 observable adenoma or cancer.

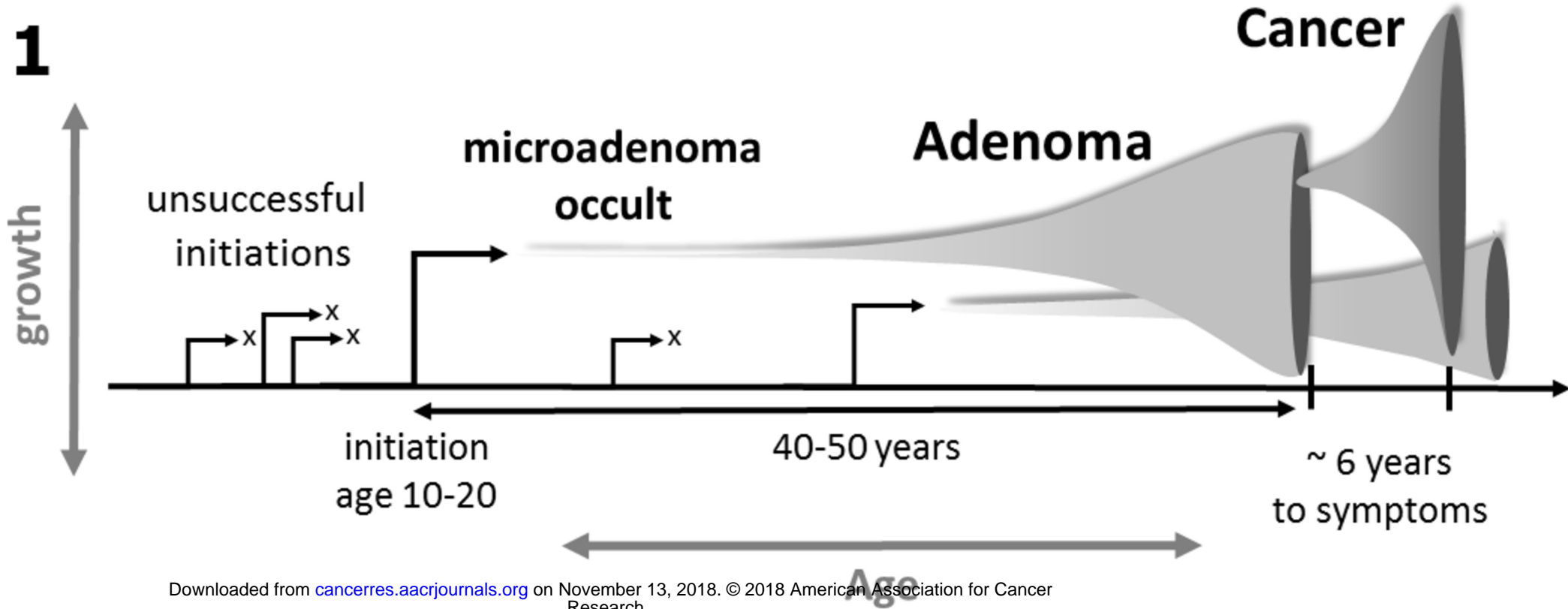
704 **Fig. 2.** Estimated CpG drift rates of 182,498 CpG probes vs the (log₂) ratio of methylation
705 variance in tumor samples relative to the corresponding variance in normal tissue samples from
706 the Luo study [11]. Variances and drift rates were computed using M-values. The drift rates
707 were estimated using linear regression of methylation vs patient age (in years). CpGs in dark
708 grey undergo significant methylomic drift (q-value <10⁻⁴), CpGs in medium grey are considered
709 static, i.e., do not show significant linear trends with patient age. The subset of CpGs marked in
710 light grey serves as a control group for the analysis of gene expression and methylomic drift
711 (see Results).

712 **Fig. 3.** Drift rate distributions in SMS for 781 CGI with a minimum of 5 identified drift-CpGs by
713 sex (solid curves) versus analogous distributions at the probe-level comprising 12,700 CpGs
714 (dashed curves).

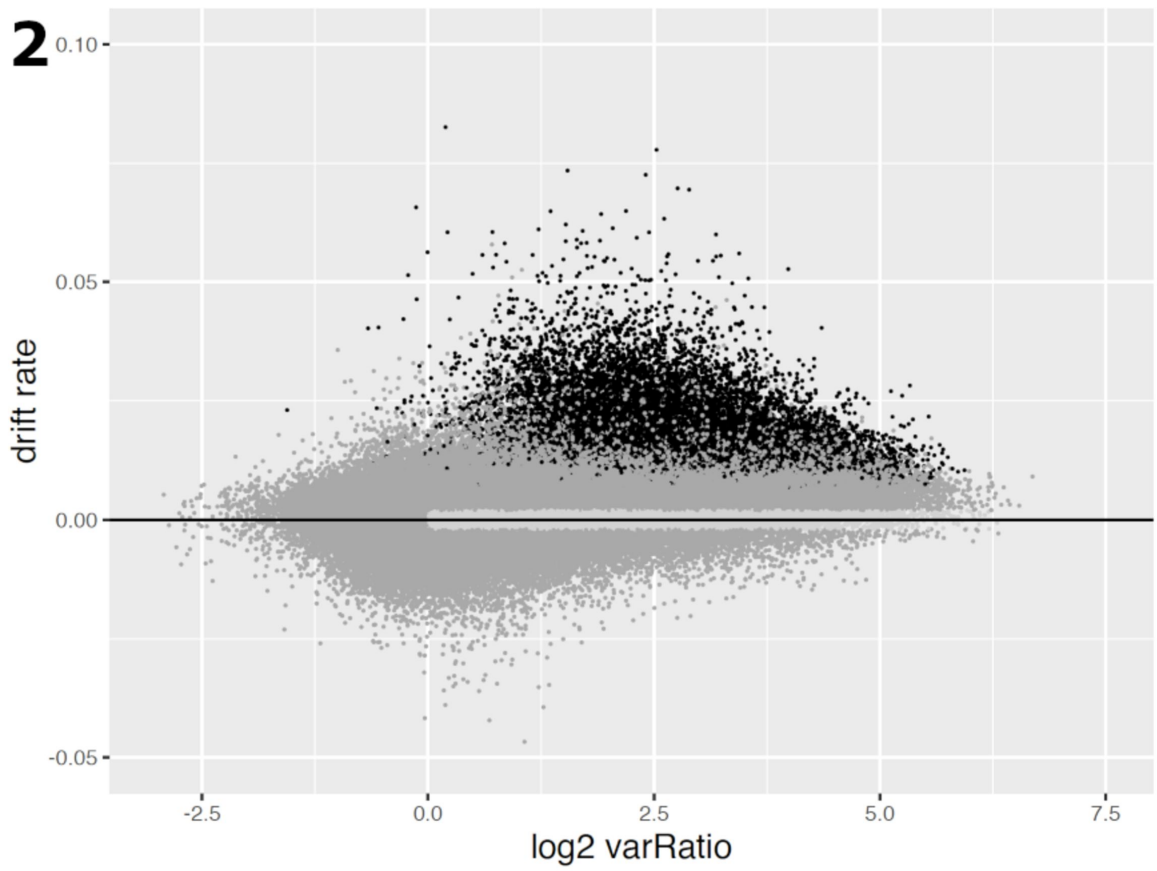
715 **Fig. 4.** Boxplots of the drift rate distributions for the same CGI as in Fig.(2), but validated in
716 samples from the GICR study for left (distal) and right (proximal) colon samples. For each group
717 the individual drift rate estimates are shown as data points. Due to small sample sizes for males
718 and females in right colon, drift rates were determined for both sexes combined in right colon.

719 **Fig. 5. A)** Expected (mean) premalignant sojourn times (in years) for males by age of cancer
720 diagnosis and anatomical site with 95% confidence bands, based on the model fits described in
721 Meza et al. [10] for UK males. **B)** Sojourn time-dependent drift curves fitted to normal/stromal
722 cell content corrected TCGA (solid symbols) and Luo (empty symbols) methylomic CGI-level
723 drift in tumors by sex and anatomical site. Regression model described in Material and
724 methods. **C, D)** same as A and B, respectively, but for females.

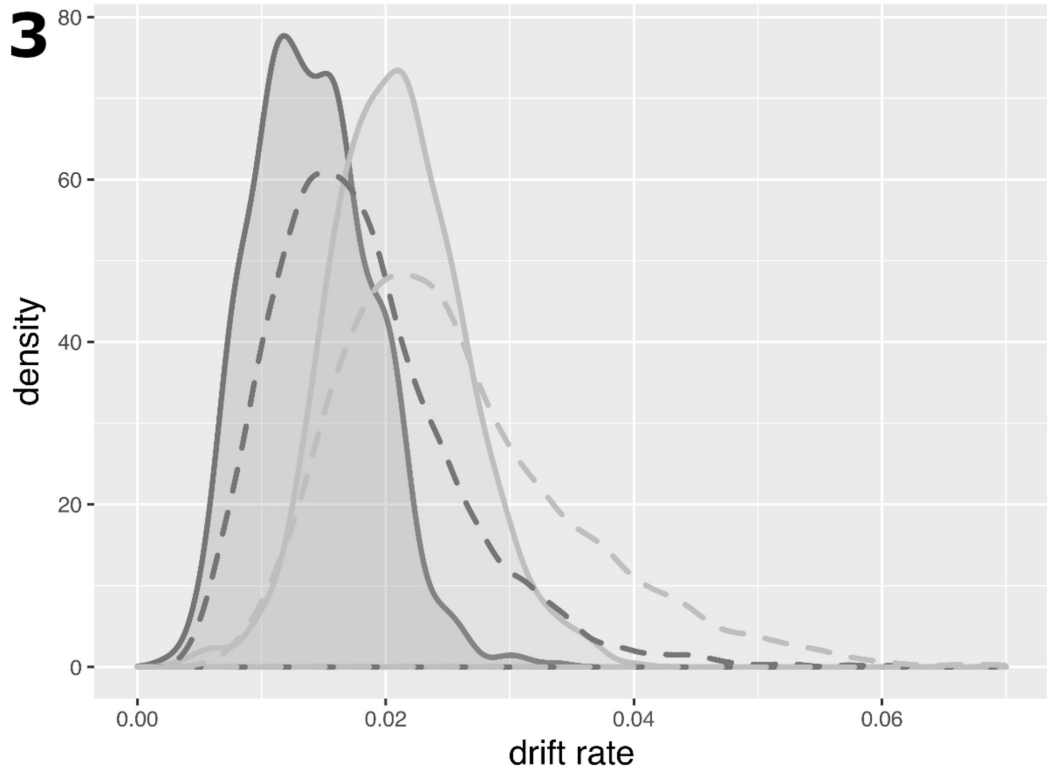
725 **Fig. 6.** Methylation heat map of 300 static CGI (top rows) and 781 drift-related CGI (bottom
726 rows) for 68 normal samples and 141 TCGA colon cancer samples (left colon only). Sample
727 groups (normal, cancers) are shown ordered by their mean island level methylation.



2

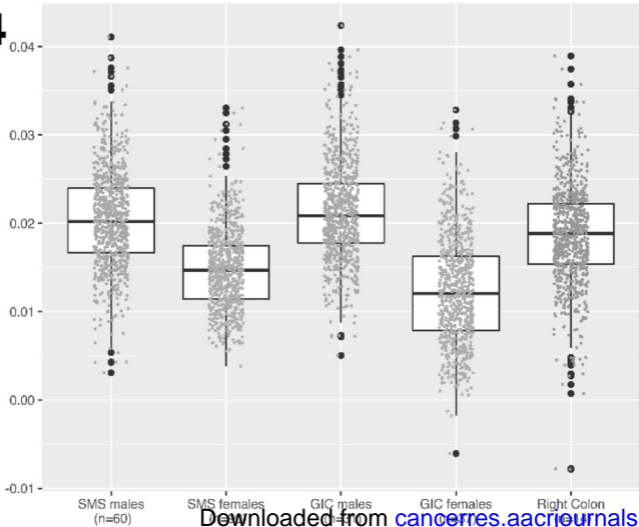


3

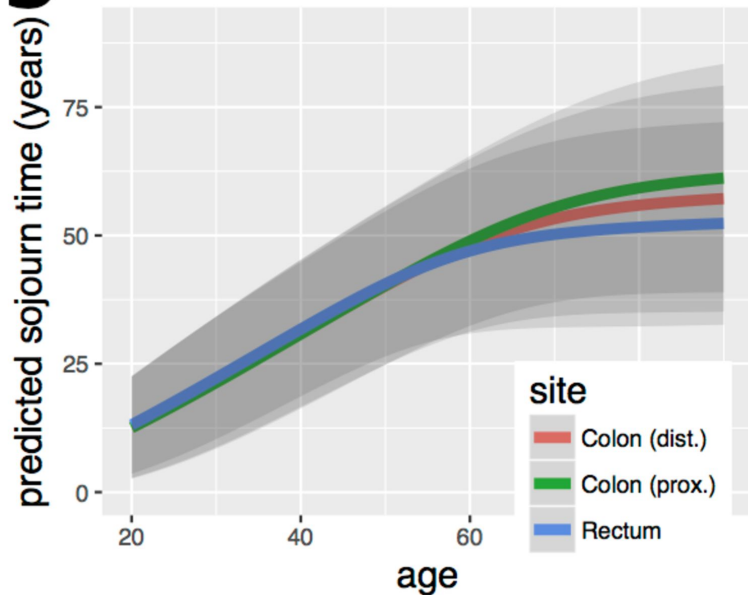


4

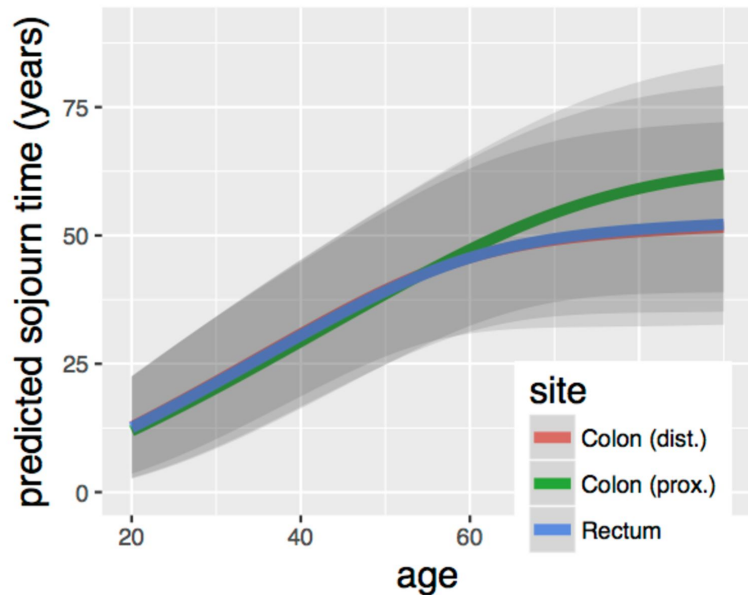
drift rates



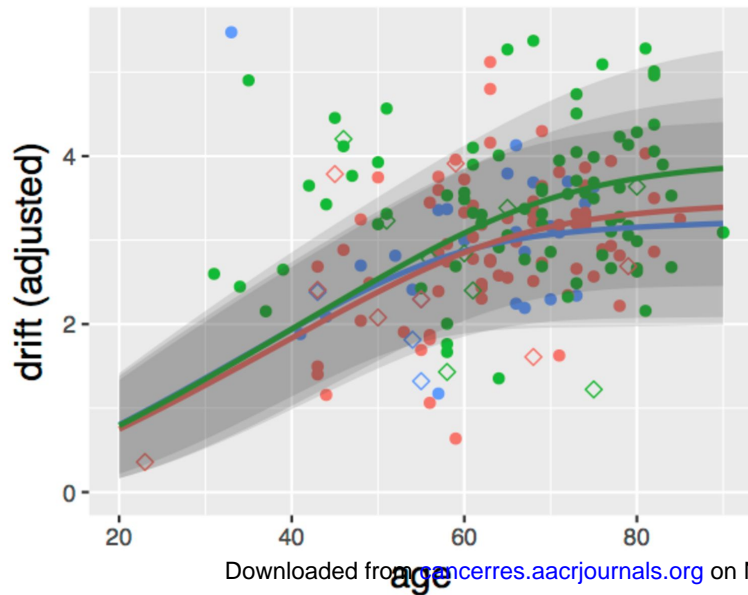
A (males)



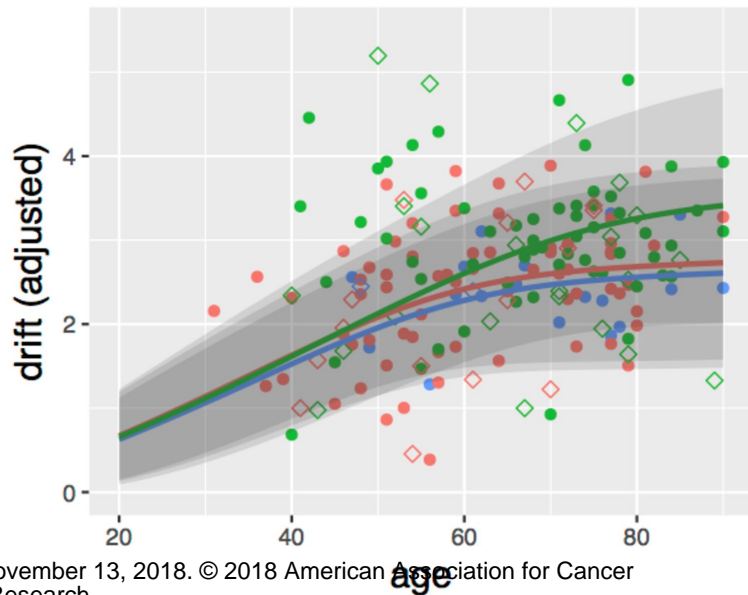
C (females)



B (males)



D (females)



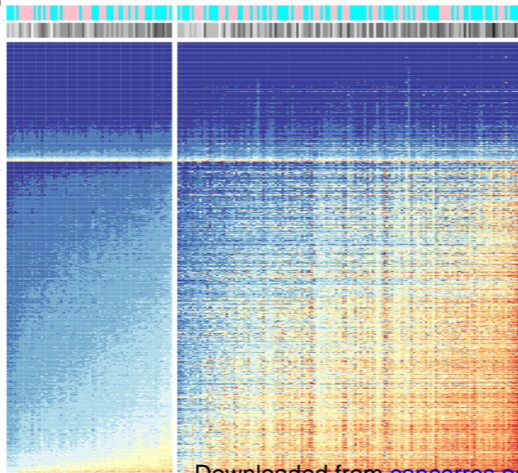
6

Normal Colon

Carcinoma (left colon)

static CGI

drift CGI

Downloaded from cancerres.aacrjournals.org

Cancer Research

The Journal of Cancer Research (1916–1930) | The American Journal of Cancer (1931–1940)

Implications of epigenetic drift in colorectal neoplasia

Georg E Luebeck, William D Hazelton, Kit Curtius, et al.

Cancer Res Published OnlineFirst October 5, 2018.

Updated version	Access the most recent version of this article at: doi: 10.1158/0008-5472.CAN-18-1682
Supplementary Material	Access the most recent supplemental material at: http://cancerres.aacrjournals.org/content/suppl/2018/10/05/0008-5472.CAN-18-1682.DC1
Author Manuscript	Author manuscripts have been peer reviewed and accepted for publication but have not yet been edited.

E-mail alerts	Sign up to receive free email-alerts related to this article or journal.
Reprints and Subscriptions	To order reprints of this article or to subscribe to the journal, contact the AACR Publications Department at pubs@aacr.org .
Permissions	To request permission to re-use all or part of this article, use this link http://cancerres.aacrjournals.org/content/early/2018/10/05/0008-5472.CAN-18-1682 . Click on "Request Permissions" which will take you to the Copyright Clearance Center's (CCC) Rightslink site.